Journal of Biomolecular NMR, 10 (1997) 21–27

J-Bio NMR 441

Alterations in chemical shifts and exchange broadening upon peptide boronic acid inhibitor binding to α-lytic protease

Jonathan H. Davis[a,*], David A. Agard[a,b,c], Tracy M. Handel[d] and Vladimir J. Basus[e,**]

[a]*Graduate Group in Biophysics and* [b]*Department of Biochemistry and Biophysics, University of California, San Francisco, CA 94143-0448, U.S.A.*
[c]*Howard Hughes Medical Institute, University of California, San Francisco, CA 94143-0724, U.S.A.*
[d]*Department of Molecular and Cellular Biology, University of California, Berkeley, CA 94720, U.S.A.*
[e]*Department of Pharmaceutical Chemistry, University of California, San Francisco, CA 94143-0446, U.S.A.*

Received 19 February 1997
Accepted 25 February 1997

Keywords: Serine protease; 3D NMR; Heteronuclear NMR

Summary

α-Lytic protease, a bacterial serine protease of 198 amino acids (19 800 Da), has been used as a model system for studies of catalytic mechanism, structure–function relationships, and more recently for studies of pro region-assisted protein folding. We have assigned the backbones of the enzyme alone, and of its complex with the tetrahedral transition state mimic *N-tert*-butyloxycarbonyl-Ala-Pro-boroVal, using double- and triple-resonance 3D NMR spectroscopy on uniformly ^{15}N- and $^{13}C/^{15}N$-labeled protein. Changes in backbone chemical shifts between the uncomplexed and inhibited form of the protein are correlated with distance from the inhibitor, the displacement of backbone nitrogens, and change in hydrogen bond strength upon inhibitor binding (derived from previously solved crystal structures). A comparison of the solution secondary structure of the uninhibited enzyme with that of the X-ray structure reveals no significant differences. Significant line broadening, indicating intermediate chemical exchange, was observed in many of the active site amides (including three broadened to invisibility), and in a majority of cases the broadening was reversed upon addition of the inhibitor. Implications and possible mechanisms of this line broadening are discussed.

Introduction

α-Lytic protease (α-LP) is an extracellular bacterial serine protease of the chymotrypsin family, produced by the soil bacterium *Lysobacter enzymogenes*. The mature enzyme is composed of 198 amino acids, has a molecular weight of 19 800 Da, and preferentially cleaves after small hydrophobic residues such as alanine. The crystal structure has been solved to 1.7 Å resolution (Brayer et al., 1979; Fujinaga et al., 1985). α-LP has been used extensively for protein engineering studies on the relationship between active site structure and function (Bone et al., 1987,1989a,b,1991b; Mace and Agard, 1995; Mace et al., 1995). Of fundamental importance in these studies has been the use of peptide boronic acid inhibitors which closely mimic the tetrahedral transition state or nearby intermediates (Kettner and Shenvi, 1984; Bone et al., 1987,1989b,1991a). While these studies suggest that protein dynamics play an important role in modulating specificity, backbone and side-chain NMR experiments will be needed to probe in detail the dynamic activity of the active site and its stabilization by peptide inhibitors.

α-LP has also proven to be extremely useful as a paradigm for the analysis of pro region-assisted protein fold-

*Present address: Harvard Medical School, Department BCMP, 240 Longwood Avenue, Boston, MA 02115, U.S.A.
**To whom correspondence should be addressed.
Abbreviations: α-LP, α-lytic protease; H-D, hydrogen–deuterium exchange; Boc-Ala-Pro-BVal, *N-tert*-butyloxycarbonyl-Ala-Pro-boroVal. Standard abbreviations are used for amino acids and NMR experiments.
Supplementary material available from the authors: two tables containing the assignments of backbone and C^{β} resonances of α-lytic protease in the absence and presence of *t*-Boc-Ala-Pro-boroVal.

TABLE 1
ACQUISITION PARAMETERS FOR EXPERIMENTS USED

Experiment	Spectrometer frequency (MHz)	Spectral width (Hz)			Complex points acquired[a]			Scans
		ω_1	ω_2	ω_3	ω_1	ω_2	ω_3	
NOESY-HSQC	600	7400 (H)	2400 (N)	8100	128	40	1024	8
HOHAHA-HMQC	500	2381 (N)	6024 (H)	6024	32	256	512	16
HNCO	600	2000 (C)	2500 (N)	9000	26	60	1024	8
HNCA	600	3333 (C)	2000 (N)	8000	64	32	512	8
HCACO	500	4650 (C)	1876 (C=O)	4000	32	64	1024	32
HN(CA)HA	500	1667 (H)	2000 (N)	7140	20	32	512	64
HNHA(HMQC)	500	2000 (N)	1818 (H)	6600	64	64	1024	32
HNHA (Gly)	600	2250 (H)	1840 (N)	8600	64	40	1024	32
H(CACO)NNH	500	1900 (N)	4600 (H)	7140	16	32	1024	32
HCA(CON)NH	500	4000 (C)	1600 (H)	7140	32	32	1024	64
HN(CO)CA	500	3333 (C)	2000 (N)	8000	32	32	512	32
HNCACB	600	6800 (C)	2500 (N)	9000	50	42	1024	8
CBCA(CO)NNH	600	9000 (C)	2400 (N)	8300	58	56	1024	16
Ref-HSQC (2D)	600	2800 (N)	8600	–	256	1024	–	64
Experiments on inhibitor complex								
HNCACB	600	1425 (N)	9000 (C)	8091	17	50	512	64
CBCA(CO)NNH	600	10000 (C)	1425 (N)	8091	59	18	512	40
H(CA)NNH-Gly	600	1425 (N)	1600 (H)	8091	17	40	512	80

[a] The final size was usually increased by linear prediction or maximum entropy, and/or zero-filling in the indirect dimensions, and the unused portions of the acquisition dimensions were trimmed away.

ing. α-LP is synthesized as a pre-pro enzyme (Silen et al., 1988) and experiments have demonstrated that the 166 amino acid N-terminal pro region is transiently required both in vivo (Silen et al., 1989) and in vitro (Baker et al., 1992) for proper folding of the mature protease domain. Refolding chemically denatured protease in the absence of the pro region leads to the formation of a stable folding intermediate with all the properties of a molten globule (Baker et al., 1992).

To study changes in the active site upon inhibitor binding, we have determined the backbone heteronuclear assignments of α-LP, both alone and complexed with the peptide boronic acid inhibitor *N-tert*-butyloxycarbonyl-Ala-Pro-boroVal (Boc-Ala-Pro-BVal, $K_i = 0.35$ nM; Kettner et al., 1988). We discuss the implications of the changes in line broadening and chemical shift observed upon inhibitor binding.

Experimental procedures

Sample preparation

α-LP was produced in its native bacterial host, *Lysobacter enzymogenes*, as described previously (Hunkapiller et al., 1973) with the following modifications: we used 0.5 g/l ^{15}N or $^{15}N/^{13}C$ Celtone (Martek) instead of casamino acids, 2.0 g/l ^{13}C fructose (Cambridge Isotope Laboratories, CIL), for uniformly ^{13}C-labeled protein instead of sucrose, and 2.4 g/l MSG (monosodium glutamate) made from either ^{15}N or $^{15}N/^{13}C$ glutamic acid (CIL). The addition of 2 ml/l 100× MEM vitamins (Sigma) produced a 10% increase in yield.

Protein was purified as previously described (Dolgikh et al., 1981; Haggett et al., 1994) except that the cation exchange chromatography step was performed using S-Sepharose (Pharmacia) with elution at pH 9.6, and an NaCl gradient of 50–200 mM. Activity was measured using the chromogenic substrate suc-Ala-Pro-Ala-pNA (Silen et al., 1989). NMR samples ranged from 0.8 to 3.5 mM, with 50–80 mM NaCl, 10 mM deuterated sodium acetate (CIL), pH 4.0 (uncorrected for isotope effects), in 92% H_2O/8% D_2O or 100% D_2O. TSP was added as an internal proton reference; ^{13}C was referenced externally to TSP in D_2O; ^{15}N was referenced to an external $^{15}NH_4Cl$ standard, which was set to 24.93 ppm relative to liquid NH_3 (Levy and Lichter, 1979).

NMR spectroscopy

NMR spectra were acquired at either 500 or 600 MHz proton frequency, and at 35 °C. The experiments used and their parameters are summarized in Table 1. Spectra of the uncomplexed form of the protein were processed using either Striker* (M. Day, unpublished results) or NMRPipe (Delaglio et al., 1995). Interactive display, bookkeeping and peak picking were performed on Sparky* (D. Kneller, unpublished results). All data processing for experiments on the complex was performed using Azara (W. Boucher, unpublished results), and interactive assignments were done using ANSIG 3.2 (Kraulis, 1989; Kraulis et al., 1994).

*For software availability, please contact Dr. T.E. Ferrin, University of California, San Francisco, CA 94143-0446, U.S.A.

Results

Assignments

The assignment process for the uncomplexed enzyme was begun by assigning arbitrary numbers to identifiable amide HN-N pairs, and trying to identify the intraresidue C^{α}, H^{α} and carbonyl from HOHAHA-HMQC (Marion et al., 1989a), HN(CA)HA (Clubb et al., 1992), HNCA, and HCACO (Ikura et al., 1990; Kay et al., 1990). Sequential connections were then provided by HNCO (Kay et al., 1990), HN(CO)CA (Bax and Ikura, 1991), and 3D HCA(CO)NNH (Boucher et al., 1992a). Although HCA(CO)NNH provided sequential correlations to most residues via the preceding H^{α}, it did not provide connections to glycine residues (of which there are 32 in α-LP). An HN(CA)HA-Gly experiment (Wittekind et al., 1993), modified to take full advantage of pulsed field gradients (Muhandiram and Kay, 1994), gave excellent results. Another generally unambiguous sequential connection was provided by the pair of experiments CBCA(CO)NNH (Grzesiek and Bax, 1992) and HNCACB (Wittekind and Müller, 1993). The inhibitor complex was then assigned using only three experiments: CBCA(CO)NNH, HNCACB, and H(CA)NNH-Gly, a 3D version of the 4D HCANNH (Boucher et al., 1992b) with timings optimized for glycine.

The experiments described above allowed us to assign 98% of the backbone spectrum of the free enzyme, and 100% of the amides in the inhibitor complex. There were three residues, G141, D142, and the active site serine S143 (S195 in chymotrypsin numbering)*, that were never found in any of the amide-detected experiments in the free enzyme, although all three appeared in the spectra of the complex. The possible sources of the missing peaks are discussed below. The supplementary material includes a practically complete list of H^{N}, N, CO, C^{α}, C^{β}, and H^{α} chemical shifts**. Figure 1 shows overlaid refocused HSQC spectra of the free enzyme and the complex, with the uncomplexed spectrum in black and the enzyme–inhibitor complex in colors. The broad amide chemical shift dispersion is readily evident; while there are many peak groups with overlapping contours, in only one or two pairs of resonances in each spectrum (A116/Q190 in free, G6/S18 and T106/N162 in complex) are the peak centers indistinguishable when separated out in a 3D experiment. The three active-site amino acids missing from the native spectrum were present in the spectrum of the complex, and are colored red in Fig. 1.

*α-LP numbering varies among different sources. For clarity, in this paper we use sequential numbering, while occasionally providing the chymotrypsin homology number for a particularly important amino acid.

**The assignments are available on the Internet, at http://util.ucsf.edu/agard/agard.html. They will also be deposited with BioMagRes Bank.

A plot comparing the change in amide chemical shift upon binding with the distance between the amide nitrogen and the nearest inhibitor heteroatom nucleus calculated from the crystal structure of the complex (Bone et al., 1987; PDB reference number 1p01) demonstrates a clear correlation between proximity to the inhibitor and the change in chemical shift (see Fig. 2A). The greatest shifts are found within about 8 Å of the bound inhibitor, but significant shifts propagate as far as 15 Å from the inhibitor. In Fig. 2A, circles represent amides weakened by exchange broadening. There is a moderate correlation between the change in chemical shift and the displacement of the amide nitrogens as calculated from the crystal structures. Wishart et al. (1991) described a linear correlation between amide ^{1}H chemical shift and hydrogen bond strength. Since several of the hydrogen bonds in the crystal structure are altered upon binding (and a new one is formed between Gly161 (G216) and the inhibitor, upper right corner of Fig. 2C), we looked for a similar correlation between the ΔH-bond strength (calculated from the two crystal structures with the program DSSP (Kabsch and Sander, 1983)) and $\Delta^{1}H$ chemical shift. The linear correlation is apparent in Fig. 2C. The points shown are those where the calculated hydrogen bond strength changed by at least 0.4 kcal.

Secondary structure evaluation

To compare the NOESY cross peaks with the crystal structure distances, we used a 3D NOESY-refocused HSQC (Marion et al., 1989b; Zuiderweg and Fesik, 1989; Davis, 1995) with a mixing time of 140 ms. The expected intensities of sequential HN-HN and H^{α}-HN_{i+1} were estimated by raising the crystal structure distances to the minus-sixth power. A plot of measured NOESY peak heights versus expected intensities revealed a linear correlation, with correlation coefficients of 0.8 (HN-HN) and 0.61 (H^{α}-HN) (data not shown). The lower correlation observed in the H^{α}-HN data is not unexpected since many of the distances are very short, leading to intense peaks and greater scatter. In no cases were there any significant violations – e.g. intense NMR peaks associated with long distances in the X-ray structure. Overall, the secondary structure found in the crystal appears to be maintained in solution. Figure 3 illustrates the intensities of the sequential backbone NOESY cross peaks.

A sample was exchanged into D_2O to determine which amide hydrogens were protected from exchange. Under conditions where the remaining amides would have protection factors of at least 1000, 128 peaks were observed, although several were weak. These residues will provide the set of useful probes for H-D exchange folding experiments, and are identified with circles in Fig. 3.

The ^{15}N line width was used to identify exchange-broadened resonances. The mean line width and its standard deviation were calculated, and 12 amides were ident-

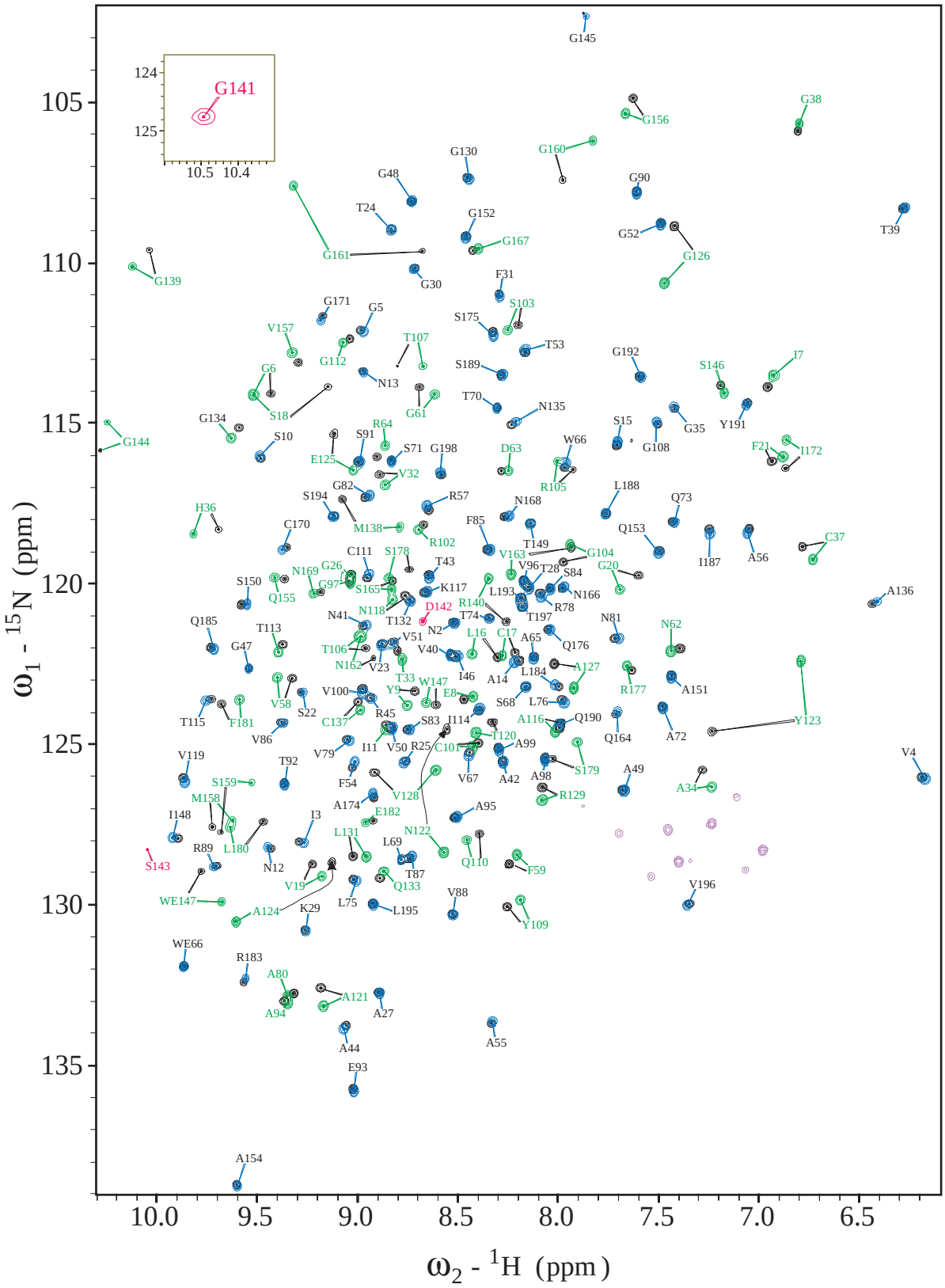

Fig. 1. ^{1}H-^{15}N correlation spectra of α-LP showing assignments of the native protein and of its complex with boronic acid inhibitor Boc-Ala-Pro-BVal. The native spectrum is shown by black peaks, and the complex overlaid in colored peaks. Blue peaks with black labels are peaks whose positions are essentially unchanged in the complex. Green peaks with green labels are those that shift in the complex, while red peaks and labels (including the one in the inset, which is shifted far up in proton frequency) are in the active site, and are only present in the spectrum of the complex. Purple peaks are arginine side-chain HN resonances that are folded in.

ified whose ^{15}N line width in a refocused HSQC spectrum of the uninhibited enzyme was greater than one standard deviation (σ) in excess of the mean. The same 12 peaks were then examined in a similar spectrum of the complex, and in most cases the broadening was significantly reduced. These results are indicated in Fig. 3 by lines and dots above the amino acid code letters.

Discussion

The spectrum of free α-LP contains 12 exchange-broadened peaks, and three other residues that are broadened to the point of invisibility. That all 15 of these correspond to residues within or near the active site seems of particular importance. When the boronic acid inhibitor is bound, six of the 12 visible broadened peaks narrow to within 1σ of the mean, two others are significantly narrowed, and all three missing resonances reappear. Only three resonances do not respond to inhibitor binding, and these are the three closest to the 1σ borderline. This result illustrates the stabilizing effect of the inhibitor on the active site of the protease.

We have considered many possible sources for the line broadening, and through a series of experiments have

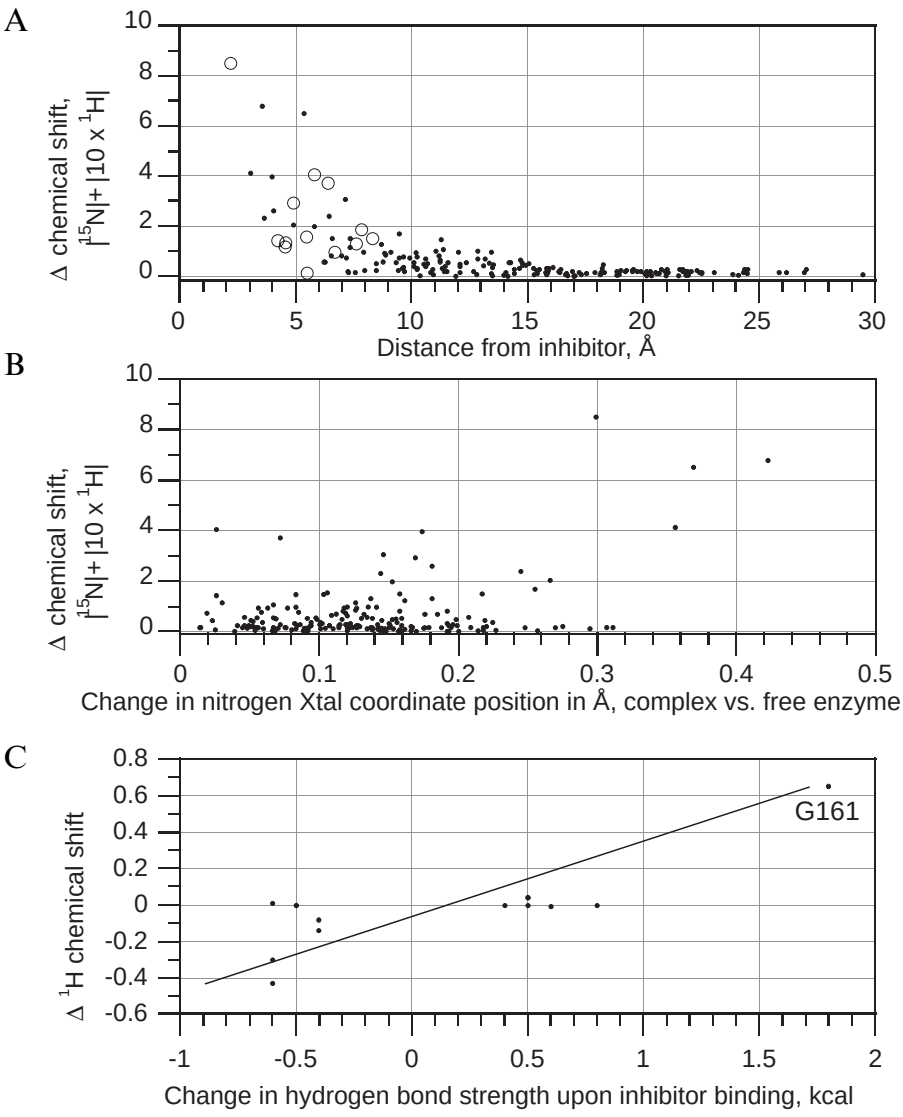

Fig. 2. Scatter plots comparing change in chemical shift upon inhibitor binding to: (A) distance of amide nitrogen from the closest inhibitor heavy atom (from the crystal structure); (B) change of nitrogen coordinate (distance in Å) from the crystal structures of the bound and unbound following superimposition based on α-carbon coordinates; and (C) change in DSSP (Kabsch and Sander, 1983) hydrogen bond strength upon binding, calculated from the native and inhibited crystal structures. In (A) and (B) the chemical shift was the sum of the nitrogen and 10× the hydrogen chemical shifts, while in (C) only the hydrogen chemical shift difference was used. In (A), circles represent amides whose resonances are weakened by chemical exchange in the unbound spectrum due to dynamics and/or peptide binding (e.g. G144, G161). This weakness is correlated with nearness to the active site and, to some degree, with chemical shift change. A moderate correlation is seen in (B) between nitrogen displacement and chemical shift change upon binding. In (C), a linear correlation is seen between H-bond strength and proton chemical shift, as described by Wishart et al. (1991).

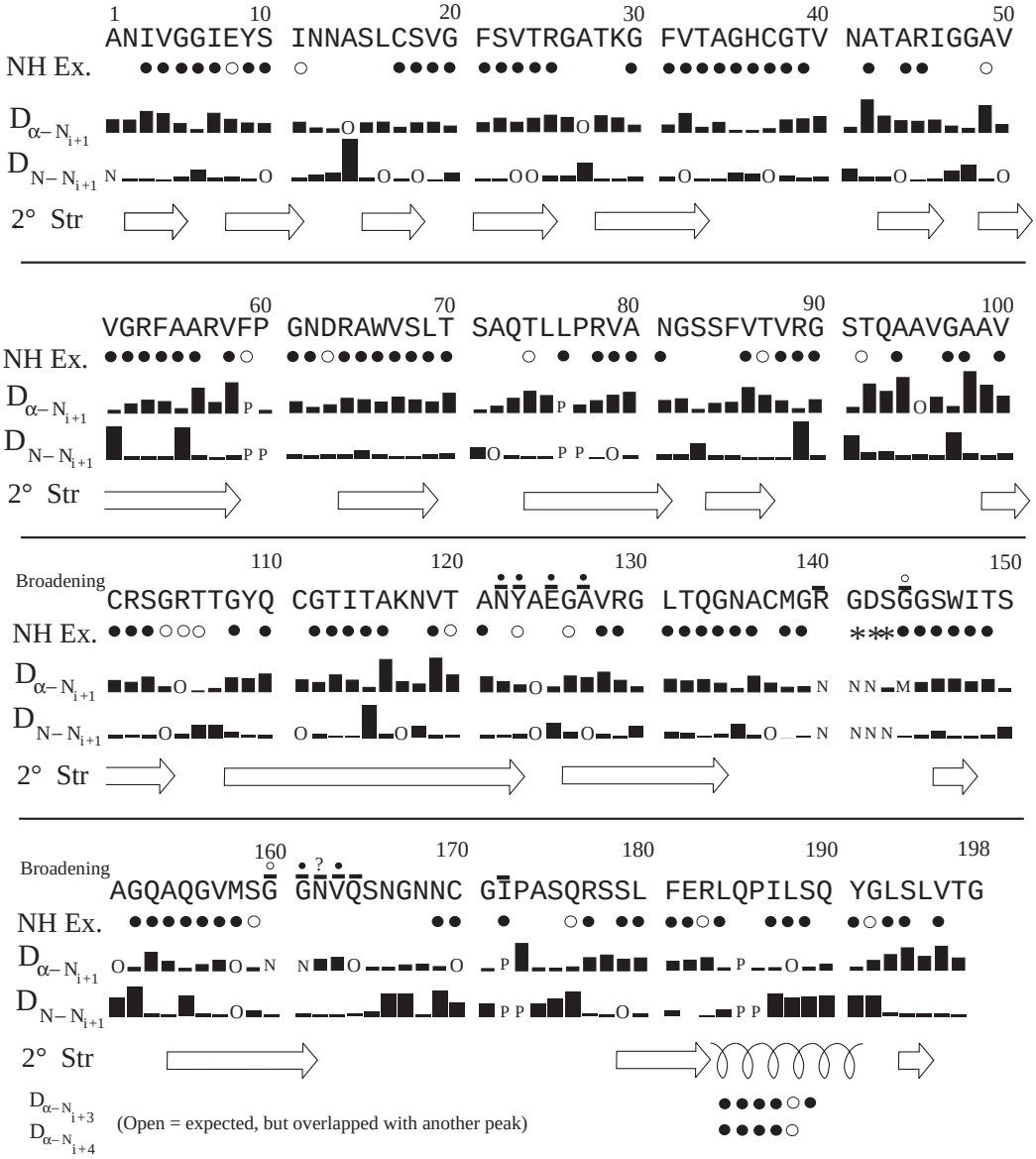

Fig. 3. Sequential connectivity diagram of the unbound enzyme. The intensity of the NOESY peak between H^{α} or HN and the following HN is indicated by the height of the bar. Secondary structure was determined from the crystal structure by DSSP (Kabsch and Sander, 1983). NH protection is indicated by circles; open circles indicate weak protection under the exchange regime described in the text. Letters in place of intensities mean the following: O = overlapped with another expected peak; N = no assignment; P = missing data due to a proline residue; M = missing peak (but expected to be weak anyway). In the bottom panel, α-helix connections between H^{α} and the amide of n+3 and n+4 residues are shown, and, aside from those missing due to overlap, all connections that are expected in an α-helix are found. The several apparent anomalies of intense HN-HN peaks within β-strands are due to twists in the backbone, but are consistent with the crystal structure distances. Residues experiencing significant ^{15}N line broadening are indicated with horizontal lines above the code letters. A solid circle above the line means the line broadening is reduced by more than one standard deviation (σ) in the spectrum of the complex, while an open circle means the reduction is between 0.5 and 1σ. N162 is overlapped in the complex.

eliminated the following mechanisms as the primary cause of line broadening: solvent exchange; histidine side-chain motion, possibly stabilized by sulfate binding to the active site; and paramagnetic metal ion binding. The most likely mechanisms that could account for the line broadening seen throughout the active site are intermediate exchange between protease and the various cleavage product peptides that invariably exist in an active protease sample, and motion on a millisecond-to-microsecond time scale. Evidence to support the peptide exchange mechanism includes the observation that many of the peaks that are most shifted upon the addition of inhibitor are also broadened (open circles in Fig. 2A), and also that older samples show worse broadening of some peaks (data not shown). However, this mechanism cannot alone account for all the line broadening, since there are some broadened peaks which show no effect from the sample age. Hence, motion on an intermediate time scale is also likely to

contribute to the observed line broadening. Interestingly, none of the crystallographic B factors for the broadened residues are in any way remarkable; in fact, the B factors for the amides of the three missing residues (G141, D142, S143) are quite low (10.5, 10.0, 12.5, respectively; Bone et al., 1987). Thus, there may be important dynamical properties of these critical active site residues that is not evident from crystallography.

The assignments reported here will allow us to perform experiments on α-LP to understand its solution structure and folding pathway, and the dynamics of its active site. Broadening of amide lines has been observed in the region bordering the substrate binding site, suggesting chemical exchange on an intermediate time scale. Determining more precisely the nature and extent of these motions should facilitate our understanding of how flexibility and dynamics relate to substrate binding and specificity. Future studies using various mutants and inhibitors will help us determine these possible roles.

Acknowledgements

This research was partially supported by the National Science Foundation Grant DMB9104794, National Institutes of Health Grant RR01695 (I.D. Kuntz, P.I.), and a grant from REAC (University of California, San Francisco) to D.A.A. and V.J.B. J.H.D. was supported in part by NIH training grant 2 T32 GM08284. D.A.A. is supported by Howard Hughes Medical Institute. T.M.H. is supported by PEW Charitable Trust Grant 93-05252. The authors would like to thank the spectroscopists at Varian, Bruker, and GE for their contribution of many high-quality spectra – in particular, thanks go to Drs. George Gray, Jerry Dallas, Clemens Anklin, and Boban John. Drs. Lewis Kay and Michael Wittekind kindly provided preprints and code for several sequences, allowing us to move faster than otherwise possible. Dr. Charles A. Kettner generously provided us with the boronic acid inhibitor. Don Kneller and Mark Day have provided most useful data analysis and processing programs. And special thanks to Dr. Dennis Benjamin, who helped in sequence implementation, programming, and generally useful discussions, and to Dr. Daina Avizonis, for good advice and support.

References

Baker, D., Sohl, J.L. and Agard, D.A. (1992) *Nature*, **356**, 263–265.

Bax, A. and Ikura, M. (1991) *J. Biomol. NMR*, **1**, 99–104.

Bone, R., Shenvi, A.B., Kettner, C.A. and Agard, D.A. (1987) *Biochemistry*, **26**, 7609–7614.

Bone, R., Frank, D., Kettner, C.A. and Agard, D.A. (1989a) *Biochemistry*, **28**, 7600–7609.

Bone, R., Silen, J.L. and Agard, D.A. (1989b) *Nature*, **339**, 191–195.

Bone, R., Fujishige, A., Kettner, C.A. and Agard, D.A. (1991a) *Biochemistry*, **30**, 10388–10398.

Bone, R., Sampson, N.S., Bartlett, P.A. and Agard, D.A. (1991b) *Biochemistry*, **30**, 2263–2272.

Boucher, W., Laue, E.D., Campbell-Burk, S. and Domaille, P.J. (1992a) *J. Am. Chem. Soc.*, **114**, 2262–2264.

Boucher, W., Laue, E.D., Campbell-Burk, S. and Domaille, P.J. (1992b) *J. Biomol. NMR*, **2**, 631–637.

Brayer, G.D., Delbaere, L.T.J. and James, M.N.G. (1979) *J. Mol. Biol.*, **131**, 743–775.

Clubb, R.T., Thanabal, V. and Wagner, G. (1992) *J. Biomol. NMR*, **2**, 203–210.

Davis, J.H. (1995) *J. Biomol. NMR*, **5**, 433–437.

Delaglio, F., Grzesiek, S., Vuister, G.W., Zhu, G., Pfeifer, J. and Bax, A. (1995) *J. Biomol. NMR*, **6**, 277–293.

Dolgikh, D.A., Gilmanshin, R.I., Brazhnikov, E.V., Bychkova, V.E., Semisotnov, G.V., Venyaminov, S.Yu. and Ptitsyn, O.B. (1981) *FEBS Lett.*, **136**, 311–315.

Fujinaga, M., Delbaere, L.T.J., Brayer, G.D. and James, M.N.G. (1985) *J. Mol. Biol.*, **184**, 479–502.

Grzesiek, S. and Bax, A. (1992) *J. Am. Chem. Soc.*, **114**, 6291–6293.

Haggett, K.D., Graham, L.D. and Whitaker, R.G. (1994) *Biotechnol. Techniques*, **8**, 203–208.

Hunkapiller, M.W., Smallcombe, S.H., Whitaker, D.R. and Richards, J.H. (1973) *Biochemistry*, **12**, 4732–4743.

Ikura, M., Kay, L.E. and Bax, A. (1990) *Biochemistry*, **29**, 4659–4667.

Kabsch, W. and Sander, C. (1983) *Biopolymers*, **12**, 2577–2637.

Kay, L.E., Ikura, M., Tschudin, R. and Bax, A. (1990) *J. Magn. Reson.*, **89**, 496–514.

Kettner, C.A. and Shenvi, A.B. (1984) *J. Biol. Chem.*, **259**, 15106–15114.

Kettner, C.A., Bone, R., Agard, D.A. and Bachovchin, W.W. (1988) *Biochemistry*, **27**, 7682–7688.

Kraulis, P.J. (1989) *J. Magn. Reson.*, **84**, 627–633.

Kraulis, P.J., Domaille, P.J., Campbell-Burk, S.L., Vanaken, T. and Laue, E.D. (1994) *Biochemistry*, **33**, 3515–3531.

Levy, G.C. and Lichter, R.L. (1979) *Nitrogen-15 Nuclear Magnetic Resonance Spectroscopy*, Wiley, New York, NY, U.S.A.

Mace, J.E. and Agard, D.A. (1995) *J. Mol. Biol.*, **254**, 720–736.

Mace, J.E., Wilk, B.J. and Agard, D.A. (1995) *J. Mol. Biol.*, **251**, 116–134.

Marion, D., Driscoll, P.D., Kay, L.E., Wingfield, P.T., Bax, A., Gronenborn, A.M. and Clore, G.M. (1989a) *Biochemistry*, **28**, 6150–6156.

Marion, D., Kay, L.E., Sparks, S.W., Torchia, D.A. and Bax, A. (1989b) *J. Am. Chem. Soc.*, **111**, 1515–1517.

Muhandiram, D.R. and Kay, L.E. (1994) *J. Magn. Reson.*, **B103**, 203–216.

Silen, J.L., McGrath, C.N., Smith, K.R. and Agard, D.A. (1988) *Gene*, **69**, 237–244.

Silen, J.L., Frank, D., Fujishige, A., Bone, R. and Agard, D.A. (1989) *J. Bacteriol.*, **171**, 1320–1325.

Wishart, D.S., Sykes, B.D. and Richards, F.M. (1991) *J. Mol. Biol.*, **222**, 311–333.

Wittekind, M., Metzler, W.J. and Müller, L. (1993) *J. Magn. Reson.*, **B101**, 214–217.

Wittekind, M. and Müller, L. (1993) *J. Magn. Reson.*, **B101**, 201–205.

Zuiderweg, E.R.P. and Fesik, S.W. (1989) *Biochemistry*, **28**, 2387–2391.